J. Physiol. (1982), **331**, *pp.* 179–210
With 15 text-figures
Printed in Great Britain

DICHROIC COMPONENTS OF ARSENAZO III AND DICHLOROPHOSPHONAZO III SIGNALS IN SKELETAL MUSCLE FIBRES

BY S. M. BAYLOR, W. K. CHANDLER AND M. W. MARSHALL

From the Department of Physiology, Yale University School of Medicine, New Haven, CT 06510, U.S.A., and the Department of Physiology, Newcastle Medical School, Newcastle-upon-Tyne

(*Received 4 January 1982*)

SUMMARY

1. Absorbance changes were measured following stimulation of single muscle fibres injected with the metallochromic indicator dye Arsenazo III. Two dye-related signals can be clearly resolved: (1) an early, transient isotropic signal that appears to be due to the formation of Ca^{2+}:dye complex and (2) a slower, transient signal that is 'dichroic' in nature. The dichroic signal is obtained by taking the difference between absorbance changes measured with light plane polarized along the fibre axis (0° light) and at right angles to the axis (90° light).

2. The time course of the dichroic signal is the same at all wavelengths employed, suggesting that a single underlying process is involved. The wavelength dependence of the magnitude of the signal is similar to that obtained for dye absorbance in a resting fibre.

3. At 570 nm, near the isosbestic wavelength for changes in H^+:dye, Mg^{2+}:dye and Ca^{2+}:dye, the dichroic signal is near maximal. The absorbance change with 0° light is positive and is about twice as large as the change with 90° light, which is negative. This finding is consistent with the idea that the dichroic signal arises from dye molecules which change their orientation in the radially symmetric muscle fibre. The direction of the change is for the dye's transition moment to become more aligned with the fibre axis during activity.

4. During a train of ten action potentials the (isotropic) Ca^{2+} transient increases in magnitude three-fold, whereas the dichroic waveform reaches a plateau value only 30–40 % larger than the single twitch value.

5. Replacing H_2O in Ringers with D_2O causes a slight reduction in the Ca^{2+} signal, reduces the dichroic signal to 0·4 times normal, and reduces tension to 0·1 times normal. Qualitatively similar reductions were found to accompany an increase in osmolality of H_2O Ringer from 1 × to 2·5 × normal.

6. Dichroic signals are also observed in fibres injected with Dichlorophosphonazo III. These are similar in many respects to the Arsenazo III dichroic signals.

7. With Arsenazo III, the dichroic signal probably arises from a reorientation of some dye molecules which are bound to one of the oriented structures in muscle. The reorientation lags the Ca^{2+} transient and may be due to a change which occurs in

the oriented structure itself. Using this idea, the Arsenazo III dichroic signal can be fitted by assuming that Ca^{2+} ions bind to receptor sites and that this binding induces the required change in the oriented structure. The analysis indicates that the hypothetical receptors have a dissociation constant for Ca^{2+} equal to 0·1–1 times the peak value of myoplasmic free [Ca^{2+}] during a twitch and an 'off' rate constant equal to 10–30 sec^{-1} at 15 °C.

INTRODUCTION

In the preceding paper (Baylor, Chandler & Marshall, 1982*b*) we showed that there is often more than a single component contributing to the change in absorbance which can be measured in stimulated muscle fibres following injection of a metallochromic indicator dye. One of these components is dichroic in nature, meaning that different absorbance changes are observed with incident light plane polarized along (0°) and perpendicular to (90°) the fibre long axis. The waveform of the dichroic signal can be obtained by taking the difference between the 0° and 90° absorbance changes, a procedure which eliminates all isotropic components. The present paper describes the properties of these signals seen with Arsenazo III and with Dichlorophosphonazo III.

With Arsenazo III it is possible to explain all the 0° and 90° changes in absorbance at different wavelengths in terms of two temporal waveforms: (1) an isotropic signal which is mainly due to the formation of Ca^{2+}:dye complex in randomly oriented dye molecules (Baylor *et al.* 1982*b*) and (2) a later dichroic signal which appears to involve a change in orientation of Ca^{2+}-free dye molecules. Although the molecular basis for the dichroic signal is not known, one possibility is that it depends on the binding of myoplasmic Ca^{2+} to Ca^{2+}-receptor sites on an oriented structure in muscle, and that this binding, in turn, results in a change in orientation of dye molecules which are bound to that structure.

Preliminary reports of some of the results have appeared (Baylor, Chandler & Marshall, 1979*a*, *b*, 1981).

METHODS

The experiments were carried out at Yale University using the methods described in Baylor, Chandler & Marshall (1982*a*, *b*).

RESULTS

Transmission changes in a fibre injected with an intermediate concentration of Arsenazo III

Fig. 1*A* shows original records taken with 0° and 90° light from a fibre containing 0·23 mM-Arsenazo III. This concentration was chosen so that the isotropic (Ca^{2+}) and dichroic signals would have similar amplitudes. For $490 \leqslant \lambda \leqslant 630$ nm the 90° trace is above the 0° trace at intermediate times and below it at later times. At 660 and 720 nm, the 0° trace is on top at both intermediate and late times.

The records in Fig. 1*B* are estimates of the dye-related absorbance changes, calculated from the records in Fig. 1*A* with a correction for changes in the intrinsic transmission properties of the fibre. The correction is the usual one (Baylor *et al.* 1982*a*, *b*), based on subtracting the records at a long wavelength where the dye does

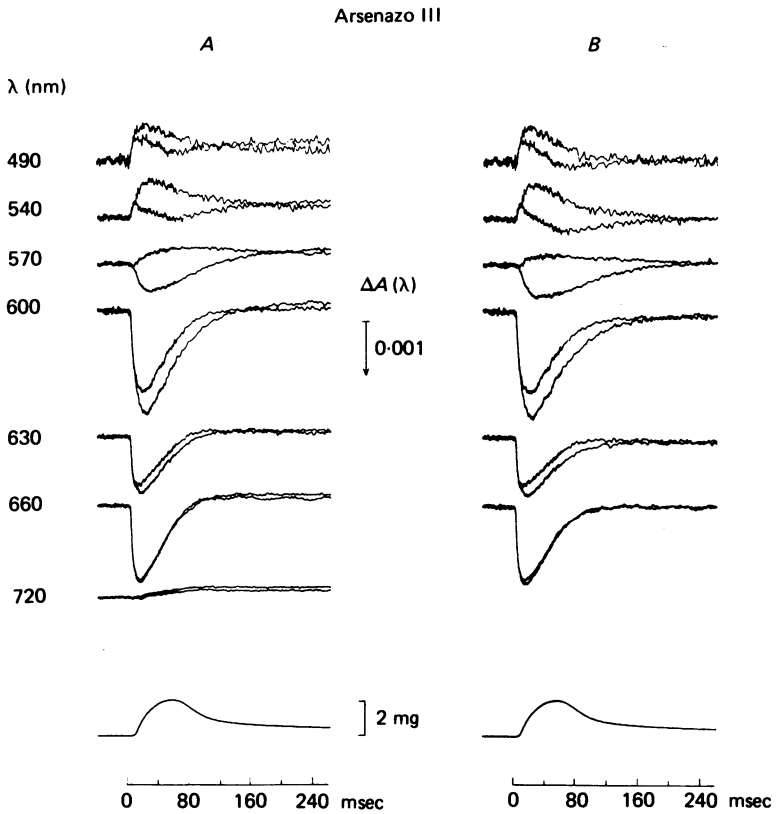

Fig. 1. Transmission signals for a fibre containing an intermediate concentration of Arsenazo III. *A*, signals using 90° and 0° light at seven different wavelengths as indicated, 10 nm filters. For λ = 490–630 nm the 90° trace is on top at the peak. For λ = 660 and 720 nm the final level of the 0° trace is on top. The records were signal averaged two to six times. During the experiment dye-related $A(570)$ varied from 0·043 to 0·047 corresponding to 0·22–0·24 mM-dye. The lowermost trace shows the average value of tension recorded during the run; the maximum variation of the peak value was 20 %. *B*, dye-related absorbance signals. i.e. same signals as in *A* but corrected for the fibre's intrinsic transmission change by subtracting the 720 nm signals scaled as $1/\lambda$. Vertical diameter, 64 μm; horizontal diameter, not measured and assumed to be 64 μm; sarcomere spacing, 3·9 μm; Ringer, 15·5 °C; fibre 010579·1.

not absorb light, in this case 720 nm, scaled according to $1/\lambda$. After correction, the final levels of the 0° and 90° traces in Fig. 1*B* are seen to superimpose, rather than cross, and to approach the base line, consistent with a final level that is nearly zero for both the dichroic signal and the isotropic signal (Baylor *et al.* 1982*b*).

It is clear from the appearance of the corrected records in Fig. 1*B* that the 660 nm traces nearly superimpose, indicating that the dye signal at this wavelength has almost no dichroic component and therefore that the isotropic and dichroic components have different wavelength dependences. The signals at other wavelengths show substantial dichroic components which are analysed in the following sections.

The dichroic signal recorded at different wavelengths

Fig. 2*A* shows the dichroic signal at different wavelengths, obtained by subtracting the 90° traces from the 0° traces in Fig. 1*B* and reversing the polarity. The subtraction automatically removes any components that are isotropic. The records all have similar waveforms. This property can be illustrated by scaling the largest record, $\lambda = 570$ nm, to the other records by a computer least squares fitting procedure and then subtracting the two records. Fig. 2*B* shows the residuals, i.e. the differences

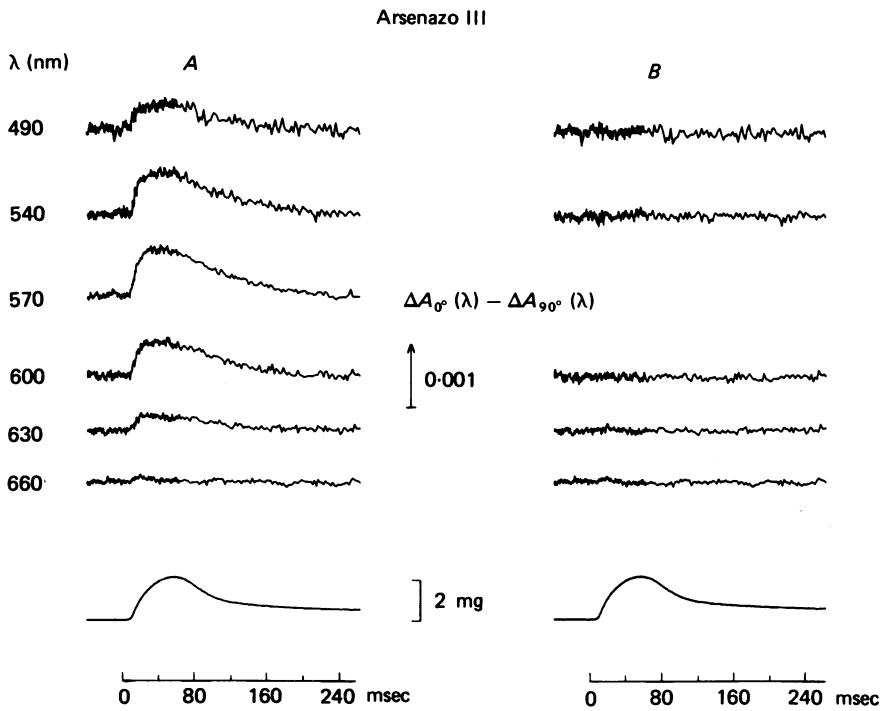

Fig. 2. Arsenazo III dichroic traces at different wavelengths. *A*, $[\Delta A_{0°}(\lambda) - \Delta A_{90°}(\lambda)]$ signals obtained by subtracting the records in Fig. 1*B* and reversing the polarity. The 570 nm trace was scaled to fit each of the other traces. The residuals are shown in *B*.

between the individual records in Fig. 2*A* and the scaled 570 nm records. Within experimental error the residuals are flat, indicating that one basic waveform and perhaps one basic process is involved in generating the dichroic signal.

Fig. 3*A* shows the scaling factors used for the fits in Fig. 2. The filled symbol gives a value of unity for $\lambda = 570$ nm and the open circles give values for the other five wavelengths. The crosses represent estimates of resting dye absorbance, divided by dye-related *A*(570). The resting data are not very reliable since the amount of dye present inside the fibre was small and the correction for the intrinsic absorbance was therefore appreciable. The curve is taken from the cuvette calibration in Fig. 1*A* of Baylor *et al.* (1982*b*) with $[Ca^{2+}] = 0$. The cuvette calibration does provide a good approximation to resting dye absorbance in fibres containing relatively large

concentrations of dye in which accurate measurements of resting dye absorbance can be made (Baylor *et al.* 1982*a*).

Fig. 3*A* shows that the wavelength dependence of the amplitude of the dichroic signal is roughly similar to that of resting dye absorbance. This finding stands in marked contrast to expectations based on changes in cation: dye complexation which

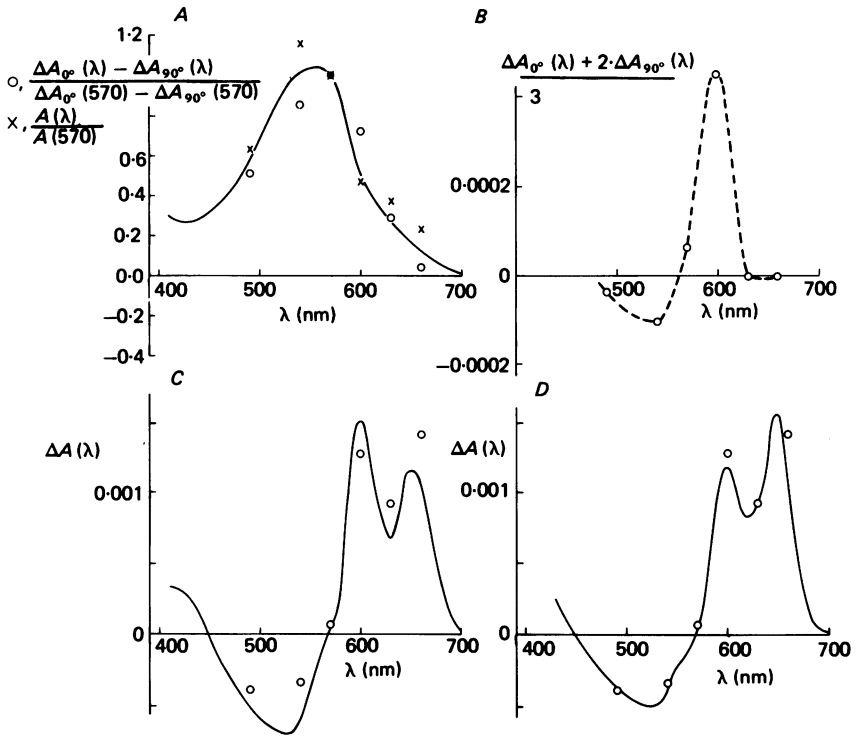

Fig. 3. Spectral properties of the dichroic and isotropic Arsenazo III signals. *A*, wavelength dependence of the magnitude of the dichroic waveform and of the resting dye absorbance. ○, scaling factors from Fig. 2*B* used to fit the 570 nm trace (●) to the other traces. The peak dichroic signal at 570 nm was $\Delta A_{0°}(570) - \Delta A_{90°}(570) = 0{\cdot}74 \times 10^{-3}$. X, resting dye absorbance scaled by dye-related $A(570)$. The smooth curve is the $[Ca^{2+}] = 0$ calibration curve drawn from Fig. 1*A* in Baylor *et al.* (1982*b*). *B*, change in absorbance of the re-orienting dye molecules. ○, experimental points $[\Delta A_{0°}(\lambda) + 2\Delta A_{90°}(\lambda)]/3$ calculated from the fits in Fig. 7*A*. According to eqn. (24) this corresponds to $A_2(\lambda) - A_1(\lambda)$, the difference spectrum of the re-orienting dye molecules. Curve drawn by eye. *C*, wavelength dependence of the magnitude of the isotropic waveform (Fig. 7*B*). The curve is drawn from Fig. 1*B* of Baylor *et al.* (1982*b*), scaled by the factor $1{\cdot}7 \times 10^{-3}$. *D*, same data points as in *C*. The curve is drawn from the curve in Fig. 7 of Baylor *et al.* (1982*b*), scaled by the factor 0·0245. From the experiment in Figs. 1 and 2.

would accompany either an increase in free $[Ca^{2+}]$ or a change in pH or free $[Mg^{2+}]$ (e.g. Baylor *et al.* 1982*b*). For such changes the 570 nm signal should vanish (i.e. 570 nm is an isosbestic wavelength) and the 540 and 600 nm signals should be in opposite directions. It is therefore apparent that an explanation other than a simple change in cation complexation is needed to explain this signal. The remaining panels in Fig. 3 will be discussed later.

Relative contributions of the 90° and 0° traces to the dichroic signal at 570 nm

The next step in the analysis was to estimate the individual contributions made by the 90° and 0° traces to the dichroic signal. The assignment should be most straightforward at 570 nm where the dichroic signal is large and the Ca^{2+} signal is minimal. Fig. 4 shows the procedure.

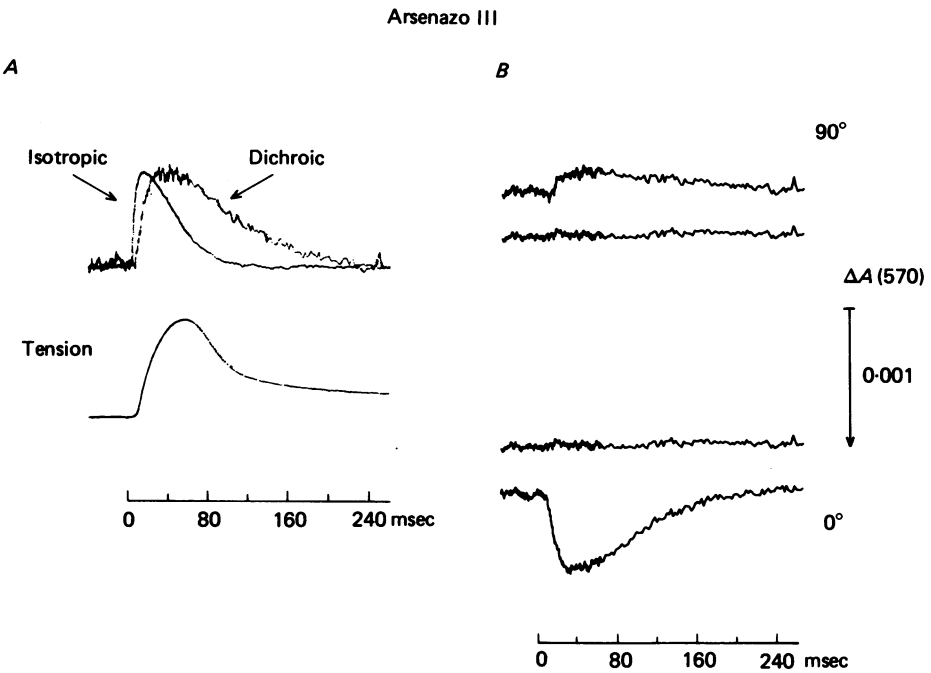

Fig. 4. Individual contributions of the 90° and 0° traces to the Arsenazo III dichroic signal at 570 nm. *A*, superimposed records of the isotropic and the dichroic signal (upper) and tension (lower). All three signals have been scaled to give the same peak value. The isotropic trace is the average of the 660 nm, 0° and 90° records in Fig. 1 *B* and the dichroic trace is the 570 nm record in Fig. 2 *A*. *B*, 90° (uppermost) and 0° (lowermost) 570 nm traces from Fig. 1 *B*. The dicroic signal in part *A* is given by the difference between these two records. The 90° and 0° records were fitted by a linear combination of the isotropic and dichroic traces in part *A* with the automatic constraint that the contribution made by the isotropic trace be the same at 90° and at 0°. The residual records associated with the fits are the middle two records in part *B*.

The upper part of Fig. 4 *A* shows two records taken from Figs. 1 and 2. The earlier record (isotropic) is the average of the two 660 nm records from Fig. 1 *B*, plotted with reverse polarity. After a short delay the dichroic signal, taken from the 570 nm record in Fig. 2 *A*, begins. Shortly thereafter tension develops as shown in the lower part of Fig. 4 *A*. It should be emphasized that the sites for optical recording and for tension generation are in different parts of the fibre so that comparisons between optical and mechanical signals should be made with caution; the optical records are obtained from the middle of the fibre whereas tension production is likely to be confined to the very ends of these highly stretched fibres (Huxley & Peachey, 1961; Baylor *et al.* 1982*a*).

The top record and bottom record in Fig. 4*B* are the 90° and 0° records at 570 nm taken from Fig. 1*B* (the difference between these records is the dichroic signal shown in Fig. 4*A*). A computer program was used to scale the dichroic trace (Fig. 4*A*) to fit the individual 90° and 0° records (Fig. 4*B*). The program was also allowed to assign a (constant) fraction of the isotropic signal (Fig. 4*A*) to the records to allow for any

TABLE 1. Fractional assignments of the isotropic and dichroic waveforms to 0° and 90° traces, 570 nm

Fibre reference (1)	Isotropic waveform (2)	Dichroic waveform	
		90° (3)	0° (4)
061478·1	0·13 (650)	−0·35	0·65
062878·1	0·00 (650)	−0·33	0·67
010579·1	0·03 (660)	−0·25	0·75
011979·1	0·03 (660)	−0·33	0·67
Mean ± S.E.M.	0·05 ± 0·03	−0·32 ± 0·02	0·68 ± 0·02

Column (1) gives the fibre reference. Column (2) gives the contribution of the isotropic waveform (650 nm or 660 nm) to the two 570 nm traces. Columns (3) and (4) (column (4) = 1 + column (3)) give the fractional contributions of the 90° and 0° traces to the total dichroic waveform. A positive number indicates an increase in absorbance. The analysis was carried out by adjusting the values in columns (2) and (3) to give a best least squares fit. All measurements were made using 10 nm filters. Arsenazo III concentration varied from 0·13 to 0·42 mM, 15–16 °C.

small amount of Ca^{2+} signal which may be present because the 570 nm filter transmits light away from the isosbestic wavelength. The computer fits were good, as is indicated by the two flat residual records shown in the middle of Fig. 4*B*. In this case the 90° trace contributed 0·25 of the magnitude of the dichroic signal and the 0° trace contributed the rest, 0·75. A small amount, 0·03, of the isotropic signal was assigned to the fit.

Fits of this type were carried out on four fibres with results tabulated in Table 1. On average the results indicate that the increase in dye absorbance seen at 0° (positive values in column 4) is about twice the decrease seen at 90° (negative values in column 3). In addition, about 0·05 of the isotropic (Ca^{2+}) signal at 650 or 660 nm was assigned to the 570 nm traces (column 2), indicating that the 570 nm filter passes some light that is not at the isosbestic wavelength for the isotropic signal.

Changes in absorbance which should accompany a change in dye orientation

The finding that dye absorbance at 0° increases while absorbance at 90° decreases suggests that the underlying mechanism may involve a change in orientation of some of the dye molecules, causing a shift of the direction of the dye's transition moment away from 90° and towards 0°. The aim of this section is to explore some of the theoretical consequences of such a shift.

Fig. 5 shows the orientation of the transition moment μ of a single dye molecule with respect to the muscle fibre. The z axis corresponds to the longitudinal axis of the fibre and lies in the plane of the paper. The x and y axes point in radial directions with the x axis lying in the plane of the paper and the y axis pointing perpendicular

to it. The transition moment makes angles α, β γ with the x, y, z axes as indicated. The experimental measurements were made by illuminating the fibre with a narrow beam of light directed along the y axis.

The following convention will be used to describe the absorption of light by one dye molecule:

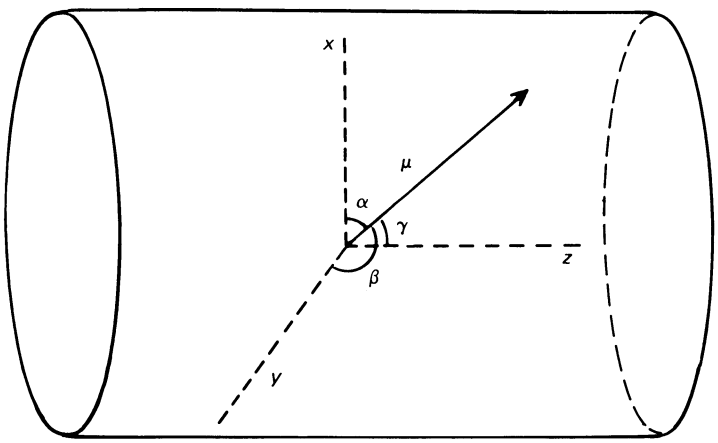

Fig. 5. Diagram showing the orientation of the transition moment μ of a dye molecule inside a muscle fibre. The z axis corresponds to the longitudinal axis of the fibre. Additional details in text.

a_x: The absorbance of incident light directed along the y axis with electric vector vibrating along the x axis (90° light).

a_y: The absorbance of incident light directed along the x axis with electric vector vibrating along the y axis.

a_z: The absorbance of incident light directed along the y axis with electric vector vibrating along the z axis (0° light).

Since the absorbance terms a_x, a_y and a_z vary as the square of the cosine of the angle between the transition moment and the direction of the electric vector (Fredericq & Houssier, 1973),

$$a_x = 3a \cos^2 \alpha, \tag{1}$$

$$a_y = 3a \cos^2 \beta, \tag{2}$$

$$a_z = 3a \cos^2 \gamma. \tag{3}$$

The factor $3a$ is a proportionality constant and is equal to the absorbance which would be observed if the direction of the transition moment were the same as the direction of the electric vector. Regardless of orientation, the identity

$$\cos^2 \alpha + \cos^2 \beta + \cos^2 \gamma = 1, \tag{4}$$

gives the relation

$$3a = a_x + a_y + a_z. \tag{5}$$

For the case of many identical molecules N, not constrained to have the same orientation of transition moments, the absorbances A_x, A_y, A_z can be defined in the same way as a_x, a_y, a_z. Since absorbance for either 90° or 0° light is additive (see below), A_x is given by the sum of all the individual a_x (which are in general not identical)

$$A_x = \sum^{N} a_x. \tag{6}$$

Similar equations hold for A_y and A_z. Eqns. (1)–(3), (5) and (6) can be combined to give

$$A_x = 3A\,\overline{\cos^2\alpha}, \tag{7}$$

$$A_y = 3A\,\overline{\cos^2\beta}, \tag{8}$$

$$A_z = 3A\,\overline{\cos^2\gamma}, \tag{9}$$

$$3A = A_x + A_y + A_z, \tag{10}$$

where $A = Na$. The bars indicate average values of the $\cos^2$ terms. If the dye molecules were randomly oriented, the average value of each $\cos^2$ term would be the same and from eqn. (4) would be equal to 1/3. In that case $A_x = A_y = A_z = A$.

Even for non-randomly oriented molecules, the radial symmetry of the fibre geometry requires that, on average, $\overline{\cos^2\alpha}$ should be equal to $\overline{\cos^2\beta}$, giving

$$A_x = A_y. \tag{11}$$

Thus, since $A_{0°} = A_z$ and $A_{90°} = A_x$, eqns. (10) and (11) give

$$A = (A_{0°} + 2A_{90°})/3. \tag{12}$$

Changes in absorbance, indicated by Δ, should follow

$$\Delta A = (\Delta A_{0°} + 2\Delta A_{90°})/3. \tag{13}$$

Eqns. (12) and (13) have general applicability in that they provide a way to eliminate any effects which are due to orientation of dye molecules. According to either equation a linear combination of twice the 90° absorbance measurement plus the 0° absorbance measurement is proportional to the absorbance a (eqn. (12)) or the absorbance change Δa (eqn. (13)) of the dye molecules themselves, independent of their orientation.

If, during a change in orientation, the absorbance properties of each dye molecule do not change (i.e. a is constant), ΔA should be zero and

$$-2\Delta A_{90°}/\Delta A_{0°} = 1. \tag{14}$$

Thus, a decrease in 90° absorbance due to a change in orientation of dye molecules should be matched by an increase in 0° absorbance which is twice as large. The average values in Table 1, columns (3) and (4), are −0·32 and 0·68 and are very close to the theoretical values $-1/3$ and $2/3$. This agreement supports the idea that the dichroic signal, at least in part, is due to reorienting dye molecules.

The additivity property, eqn. (6), strictly holds only if the polarization form of the light is not altered as the light passes through the fibre. For radially symmetric structures this condition applies

to 0° and to 90° light (which is the reason why these orientations were chosen) provided the structure does not show optical rotation (optical activity). This appears to be the case in non-injected fibres since both the resting light intensity and the active change recorded with the fibre placed between crossed polarizers vanishes when the angles are 0° and 90° (Baylor & Oetliker, 1977). Checks were not made on injected fibres but there is no reason to expect the presence of dye to induce optical rotation.

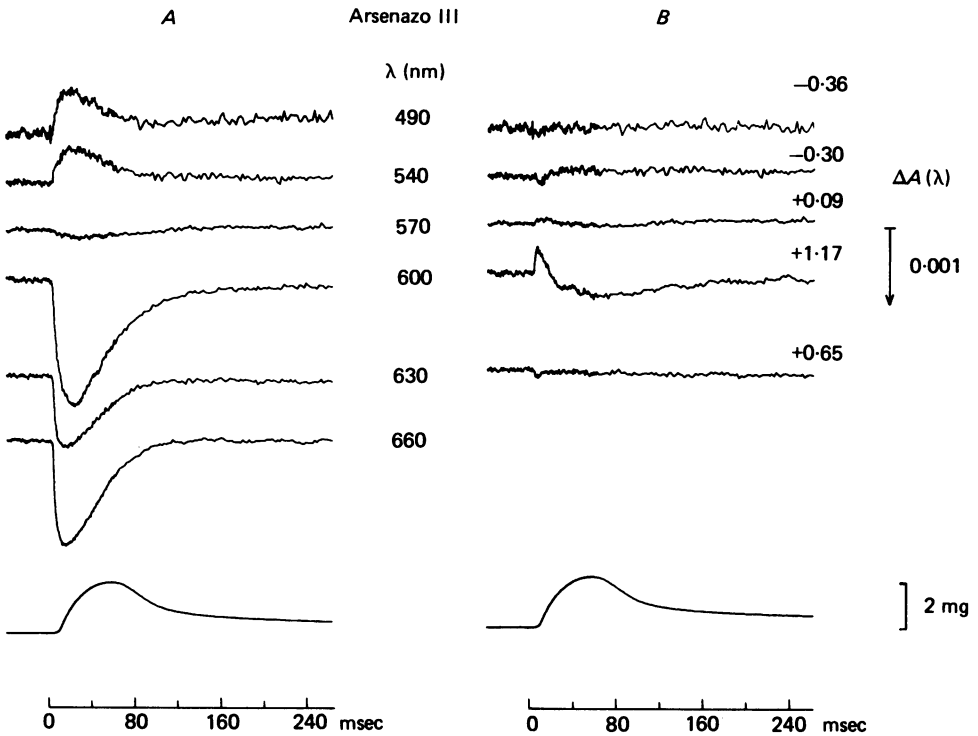

Fig. 6. Analysis of Arsenazo III signals assuming that the dichroic signal is due solely to a change in dye orientation. *A*, records of $[2\Delta A_{90°}(\lambda)+\Delta A_{0°}(\lambda)]/3$ obtained from Fig. 1*B*. The re-orientation component of the dichroic signal has been eliminated by the 2:1 weighting as set by eqn. (14). The 660 nm record was scaled to fit each of the other records. The residuals are shown in *B* with scaling factors indicated. From the experiment in Figs. 1–2.

Analysis of Arsenazo III signals on the assumption that the dichroic signal arises from a change in dye orientation alone

The contributions of the 90° and 0° traces to the total dichroic signal (Fig. 4 and Table 1) were determined using the 570 nm interference filter, selected because the passband is closest to the isosbestic wavelength. This was the obvious starting point since the dichroic signal was large and the isotropic Ca^{2+} signal was small.

Eqns. (13) and (14) can now be used to see whether the 90° and 0° signals at all wavelengths in Fig. 1*B* can be explained by contributions from one isotropic waveform plus one dichroic waveform which is produced solely by a change in dye orientation. The procedure used to test this idea was to use the relationship in eqn. (14) to eliminate the re-orientation dichroic component at each λ and to see whether

the remaining 'isotropic' component has the same waveform at all λ. The 'isotropic' signals so obtained, Fig. 6*A*, appear to have similar waveforms. A more exact comparison can be made by scaling the 660 nm record to fit each of the other records. The residuals are shown in Fig. 6*B* with the appropriate scaling factors indicated alongside each trace. The fits are reasonably good except for the record at 600 nm, where the discrepancy is too large to be attributed to experimental error.

The lack of perfect fit based on a single isotropic change in dye absorbance and a re-orientation of some dye molecules indicates, according to eqn. (13), that there must be another change in dye absorbance which has not been included in the analysis. This additional component could represent either a change in absorbance of the re-orienting dye molecules or a second isotropic change. However, a second isotropic change is not seen in more heavily injected fibres in which the isotropic signal is much larger than the dichroic signal. In this case, the isotropic signals all follow approximately the same time course (Fig. 5 in Baylor *et al.* 1982*b*). Although it is possible that a second isotropic signal is revealed at low dye concentration, it seems more likely that the additional change in absorbance occurs in the re-orienting dye molecules themselves.

Signals which would accompany changes in both the orientation and the absorbance spectrum of dye

It was therefore of interest to extend the previous analysis to include changes in the absorbance properties (as well as changes in orientation) of the re-orienting dye molecules. Subscripts 1 and 2 will be used to denote two different absorbance states, 'resting' and 'active', respectively.

Suppose N molecules have total absorbance $3A_1$ at rest and an average orientation along the z axis $\overline{\cos^2\gamma_1}$. The contribution that these molecules make to resting absorbance is given by

$$A_{1,0^\circ} = 3A_1\,\overline{\cos^2\gamma_1}, \tag{15}$$

$$A_{1,90^\circ} = 3A_1[(1-\overline{\cos^2\gamma_1})/2]. \tag{16}$$

During activity suppose that A_1 changes to A_2 and $\overline{\cos^2\gamma_1}$ to $\overline{\cos^2\gamma_2}$, giving

$$A_{2,0^\circ} = 3A_2\,\overline{\cos^2\gamma_2}, \tag{17}$$

$$A_{2,90^\circ} = 3A_2[(1-\overline{\cos^2\gamma_2})/2]. \tag{18}$$

The changes which will be measured are

$$\Delta A_{0^\circ} = A_{2,0^\circ} - A_{1,0^\circ} \tag{19}$$

$$= 3[A_2\,\overline{\cos^2\gamma_2} - A_1\,\overline{\cos^2\gamma_1}], \tag{20}$$

$$\Delta A_{90^\circ} = A_{2,90^\circ} - A_{1,90^\circ} \tag{21}$$

$$= \tfrac{3}{2}[(A_2-A_1) - (A_2\,\overline{\cos^2\gamma_2} - A_1\,\overline{\cos^2\gamma_1})]. \tag{22}$$

Taking the ratio of eqns. (22) and (20) gives

$$-2\Delta A_{90^\circ}/\Delta A_{0^\circ} = 1 - \frac{A_2-A_1}{A_2\,\overline{\cos^2\gamma_2} - A_1\,\overline{\cos^2\gamma_1}}. \tag{23}$$

The right hand side reduces to unity if there is no change in A (i.e. $A_2 = A_1$), in agreement with eqn. (14). In other cases, however, it is clear that ratios of $\Delta A_{90°}/\Delta A_{0°}$ different from $-1/2$ might occur.

Arsenazo III signals as linear combinations of the isotropic and dichroic waveforms

The purpose of this section is to see whether good theoretical fits can be obtained for 0° and 90° traces at all wavelengths using a single isotropic waveform and a single

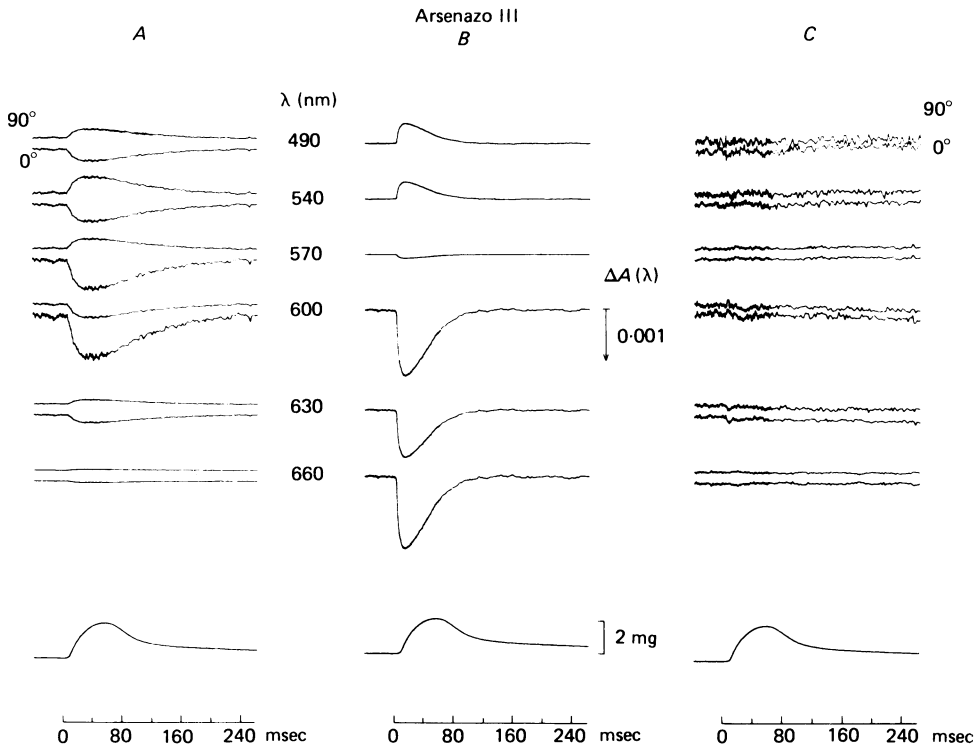

Fig. 7. Arsenazo III signals as linear combinations of the dichroic and isotropic signals. The traces in Fig. 1 *B* were each fitted by a linear combination of the dichroic and isotropic waveforms in Fig. 4 *A*. *A* and *B*, contributions made by the dichroic and isotropic waveforms to each trace. *C*, residuals. From the experiment in Figs. 1 and 2.

dichroic waveform, but without the restriction that the dichroic ratio $\Delta A_{90°}/\Delta A_{0°} = -1/2$. As shown in the preceding section, removal of the $-1/2$ restriction allows for changes in the absorbance spectrum of the re-orienting dye molecules. The question, then, is whether all the traces in Fig. 1 *B* can be fitted by a linear combination of the isotropic and dichroic waveforms that are shown in Fig. 4 *A*.

A least squares computer program was used to make the fits. For $\lambda \neq 570$ nm the additional restriction was imposed that the isotropic assignments must be the same at 0° and 90° (this condition automatically applies at $\lambda = 570$ nm since the dichroic waveform chosen for the fits is the difference between the 0° and 90° traces at 570 nm).

Fig. 7*A* shows the amount of dichroic waveform assigned to the 0° and 90° traces at each wavelength. The traces at $\lambda = 570$ nm are the same as those in Fig. 4*B*. Fig. 7*B* shows the isotropic waveform assignments. Fig. 7*C* shows the residuals, i.e. the difference between the original records in Fig. 1*B* and the combined dichroic and isotropic records from Fig. 7*A* and *B*. The residuals are flat within the error of the measurements and indicate that linear combinations of the two chosen waveforms fit the data. In a general way this means that all the signals can be explained on the basis of two temporally distinct processes. In terms of the records shown in Fig. 6*A*, this means that all changes in absorbance which occur in the dye molecules themselves, independent of orientation, can be fitted by two temporal processes. One has the waveform shown by the 660 nm isotropic signal and the other has the waveform shown by the 570 nm dichroic signal.

The peak amplitudes of the isotropic signal in Fig. 7*B* are plotted as circles in Fig. 3*C* and *D*. The wavelength dependence is very similar to that described for the isotropic Ca^{2+} signal in a more heavily injected fibre (e.g. Figs. 6 and 7 in Baylor *et al.* 1982*b*). The normalized Ca^{2+}-difference curve from Fig. 1*B* of Baylor *et al.* (1982*b*), scaled by the factor $1{\cdot}7 \times 10^{-3}$, is included in Fig. 3*C* for comparison. It corresponds to the change that would be expected on the basis of 1:1 stoichiometry, for dye concentrations from 30 μM to 1 mM, if 0·038 of the Arsenazo III were bound to Ca^{2+} [0·038 is obtained by dividing the factor $1{\cdot}7 \times 10^{-3}$ by 0·0445, the average value of $A(570)$ for this experiment]. The Ca^{2+}-difference curve from Fig. 7 of Baylor *et al.* (1981*b*), scaled by 0·0245, is drawn in Fig. 3*D*. This curve, determined at very low dye concentration, provides a better fit to the isotropic component than the curve in part *C*. The scaling factor corresponds to 0·034 of the Arsenazo III being bound to Ca^{2+}, using the same method of calculation as was used for part *C* ($0{\cdot}062 \times 0{\cdot}0245 \div 0{\cdot}0445$). As was concluded previously from experiments on more heavily injected fibres (Baylor *et al.* 1982*b*), the wavelength dependence of the isotropic component makes it likely that this component in the records in Fig. 1*B* arises primarily from formation of Ca^{2+}:dye complex produced by an elevation of myoplasmic free $[Ca^{2+}]$.

Absorbance changes in the dye molecules which produce the dichroic signal

The 0° and 90° components of the dichroic signal in Fig. 7*A* can be further analysed by combining eqns. (20) and (22),

$$A_2 - A_1 = (\Delta A_{0°} + 2\Delta A_{90°})/3 \tag{24}$$

and

$$A_2(\overline{\cos^2 \gamma_2} - 1/3) + A_1(1/3 - \overline{\cos^2 \gamma_1}) = (2/9)\,(\Delta A_{0°} - \Delta A_{90°}). \tag{25}$$

Eqn. (24), which is essentially the same as eqn. (13), provides a way to estimate the change in absorbance of the re-orienting dye molecules. This spectrum is plotted in Fig. 3*B*. The units correspond to the change in absorbance that would be measured if the dye molecules which produce the signal were all randomly oriented (which they are not). The curve shows a minimum around 550 nm, a peak near 600 nm and an isosbestic point between 540 and 570 nm. The magnitude of the peak at 600 nm is about one third the magnitude of the 600 nm isotropic signal, shown in parts *C* and

D. In part *B* there is no indication of the two peaks at 600 and 650 nm which are characteristic of the Ca^{2+}-difference spectrum.

On the other hand, the wavelength dependence of the magnitude of the dichroic signal (Fig. 3*A*) should obey eqn. (25). Two limiting cases of this equation will be considered later when the molecular basis of the dichroic signal is discussed. The first case is that the dye molecules in question are randomly oriented at rest and become oriented during activity. In this case $\overline{\cos^2 \gamma_1} = 1/3$ and the spectrum of the $\Delta A_{0°} - \Delta A_{90°}$ signal is proportional to A_2, the absorbance spectrum of the oriented molecules; also, one obtains $\overline{\cos^2 \gamma_2} > 1/3$. In the other extreme, one might imagine that dye goes from an oriented state at rest to a non-oriented state during activity. In this case $\overline{\cos^2 \gamma_2} = 1/3$, $\overline{\cos^2 \gamma_1} < 1/3$ and the spectrum is proportional to A_1.

Therefore, if either the resting or the active state involves randomly oriented dye molecules, the spectrum of the dichroic signal is exactly proportional to the absorbance spectrum of the dye in the other, oriented state. If, as seems equally likely, both states are oriented, the spectrum includes contributions from A_1 and A_2, each weighted according to a factor $(\overline{\cos^2 \gamma} - 1/3)$ which indicates how much the orientation deviates from being purely random.

Effect of Arsenazo III concentration on the dichroic signal

Since the presence of oriented dye molecules may be due to the binding of dye to an oriented structure, it was of interest to determine the effect of Arsenazo III concentration on the dichroic signal. Fig. 8 shows traces from three experiments in which it was possible to record signals as dye concentration varied by two-fold or more. Part *A* shows six optical records taken 24–48 min following the completion of dye injection. During this time dye-related $A(570)$ decreased from 0·062 to 0·029 owing to longitudinal diffusion of dye along the fibre. The range of values for $A(570)$ corresponds to Arsenazo III concentrations 0·23–0·11 mM. The signals have essentially identical waveforms although the last two records, taken with a 10 nm filter, are somewhat noisier than the first four records, taken with a 30 nm filter which passes more light.

Panel *B* shows a similar series of records, beginning with dye-related $A(570) = 0·106$, dye concentration 0·43 mM, and ending with $A(570) = 0·034$, dye concentration 0·14 mM. In this case the waveform changed slightly with time. The upper records show a small, early downward signal which decreased with time. Concomitantly, the position of the peak of the waveform shifted to the left, possibly due to the disappearance of the early downward component.

Panel *C* of Fig. 8 shows the third experiment. The first record was taken 20 min following dye injection, dye-related $A(570) = 0·052$, dye concentration 0·23 mM. This waveform resembles those in part *A* and the last two records in part *B*. The fibre was re-injected and records were taken at 11 and 33 min following the second injection. During this time the dye concentration changed from 0·54 mM ($A(570) = 0·125$) to 0·37 mM ($A(570) = 0·086$). At 11 min there was a large, early downward component and a depressed peak level. At 33 min the early component decreased and the peak level increased, although the waveform was still considerably different from the top record taken 20 min following the first injection.

The fibre was then injected a third time and 50 min later the lowermost optical

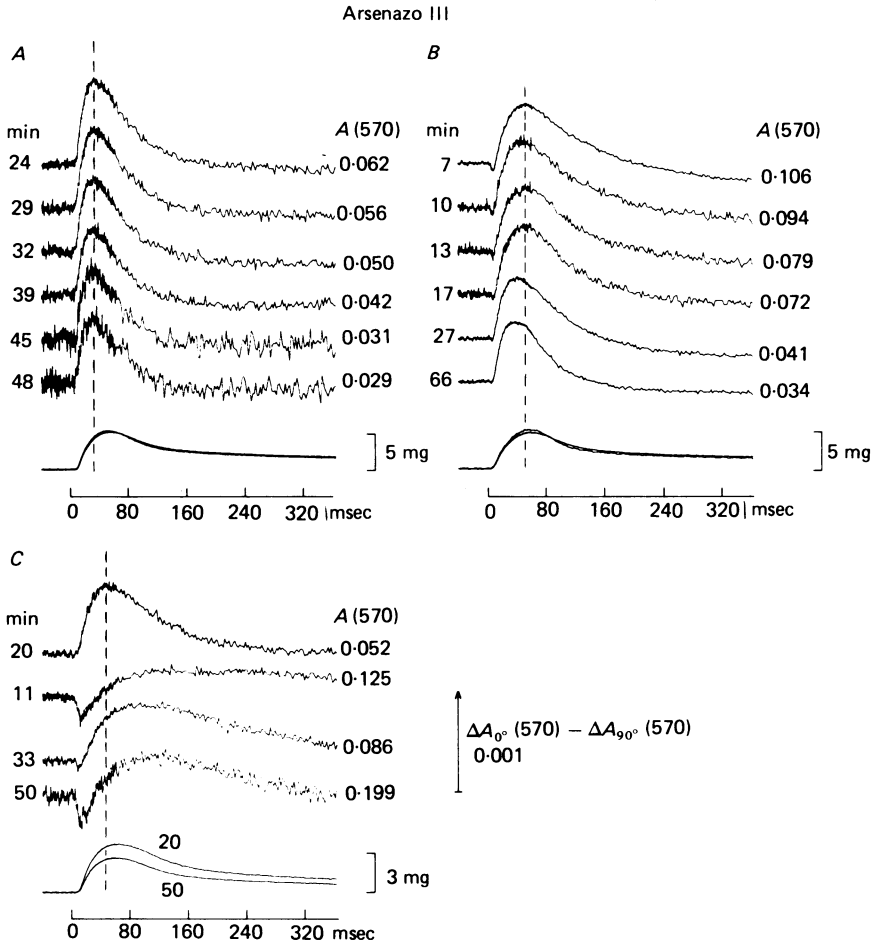

Fig. 8. Effect of Arsenazo III concentration on the 570 nm dichroic signal. *A*, six records taken at different times (indicated on left) following dye injection. Dye-related *A*(570) is indicated on right. The first four records were taken with a 30 nm filter and the last two records with a 10 nm filter. The two superimposed tension traces were taken with the first and sixth optical records. The dashed vertical line is drawn through the peak of the first optical signal. Vertical diameter, 74 μm; horizontal diameter, 88 μm; sarcomere spacing, 3·9 μm; Ringer, 15·0–15·7 °C; fibre 061478·1. *B*, similar protocol to *A*. 30 nm filters used throughout. Vertical and horizontal diameters, 82 μm; sarcomere spacing, 4·3 μm; Ringer, 15·9–16·4 °C; fibre 061578·1. *C*, records from a fibre that was injected three times (10 nm filters). The first trace was taken 20 min following the first injection. The next two traces were taken 11 and 33 min following the second injection. The fourth record was taken 50 min following the third injection. The two tension records were associated with the first and fourth optical records as indicated. Vertical diameter, 69 μm; horizontal diameter, 77 μm; sarcomere spacing, 3·9 μm; Ringer 15·5–15·7 °C; fibre 071378·1. In *A*–*C* each record represents the difference between one to four signal-averaged 0° and 90° traces.

record was taken, dye-related $A(570) = 0{\cdot}199$, 0·86 mM-dye. The early downward component again became apparent and the peak was reduced.

Fig. 9 shows peak values of the dichroic signal plotted against dye-related $A(570)$/diameter, or concentration of Arsenazo III, from all the experiments. The three fibres in Fig. 8 are indicated by ● (A), ■ (B) and ◆ (C). These have been

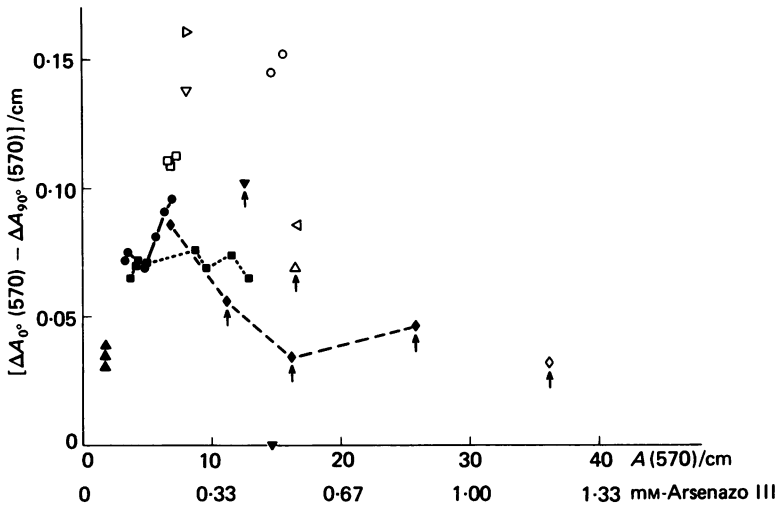

Fig. 9. Magnitude of the 570 nm dichroic signal measured at different concentrations of Arsenazo III. Abscissa gives dye-related $A(570)$ divided by fibre horizontal diameter on upper label and concentration of Arsenazo III on lower label. Ordinate gives peak value of the dichroic signal, corrected for the intrinsic dichroic signal of the fibre and divided by horizontal diameter. Each symbol is a different fibre. The filled symbols are from experiments done in June and July, 1978; the open symbols are from experiments done in December, 1978 and January, 1979. Arrows mark data points in which the peak of the dichroic signal occurred after the peak of tension. In all other records the dichroic trace peaked before tension. Continuous, dashed and dotted lines connect points from the three experiments in Fig. 8 (●, A; ■, B; ◆, C). Horizontal diameters, 53–105 μm; sarcomere spacings, 3·9–4·3 μm; Ringer 15–17 °C.

connected by line segments. The other measurements were from fibres in which there was little variation in dye concentration during the time that dichroic signals were recorded. At dye concentrations greater than 0·4 mM the dichroic signal frequently peaked after tension, as was noticed in the lower three traces in Fig. 8C. These experimental points are marked by an arrow in Fig. 9. Although the cause of the later dichroic signal is not known, it may be related to the longer lasting Ca^{2+} signal which is seen at higher dye concentrations (Fig. 3 in Baylor *et al.* 1982*b*) or to the appearance of a downward component of the dichroic signal (Fig. 8B and C of this paper).

The data in Fig. 9 were obtained in two different sessions, June–July 1978 and December 1978–January 1979. The first group of fibres appeared to give somewhat smaller signals than the second group. For this reason filled symbols have been used to denote values from the first group and open symbols have been used for values from the second group. In each group there is a slight indication that the amplitude of the dichroic signal may be approximately constant for 0·1–0·4 mM-Arsenazo III

and may decrease at higher concentrations. The reduction appears to be associated with a change in waveform, namely the appearance of an early downward component and a later time-to-peak (Fig. 8).

Although the results show variability the point that does seem clear is that waveforms of the dichroic signal recorded at dye concentrations between 0·06 and

TABLE 2. Arsenazo III resting dichroism

Fibre reference (1)	Horizontal diameter (μm) (2)	A(570) (3)	Dye concentration (μM) (4)	$A_{0°}(\lambda)-A_{90°}(\lambda)$ 570 nm (5)	720, 750 nm (6)	(5)−(6) (7)	Dye concentration (μM) (8)
061578·1	82	0·07–0·09	285–366	0·010	0·011	−0·001	−1
062678·2	92	0·02–0·03	72–109	0·014	0·013	0·001	1
062878·1	53	0·07	440	0·014	0·007	0·007	15
071378·1	77	0·09–0·12	390–519	0·018	0·013	0·005	7
010579·1	64	0·04–0·05	208–260	−0·005	0·008	−0·013	−23
010579·2	69	0·11	531	0·029	0·015	0·014	23
011979·1	105	0·09	286	0·020	0·012	0·008	8
Mean ± S.E.M.						0·003 ± 0·003	4 ± 5

Column (1) gives fibre reference; (2) gives fibre horizontal diameter; (3) gives dye-related A(570), average of 0° and 90° measurements; (4) gives dye concentration, calculated from (2) and (3) using $\epsilon(570) = 3 \times 10^4$ M^{-1} cm^{-1}; (5) and (6) give $A_{0°}(\lambda)-A_{90°}(\lambda)$ values for 570 nm and for 720 or 750 nm; values in column (7) represent the difference between (5) and (6); column (8) gives the concentration of dye molecules, oriented along the fibre axis, which would account for the values in column (7). The latter calculation is based on $\epsilon(570) = 3 \times 10^4$ M^{-1} cm^{-1} for randomly oriented Arsenazo III molecules which gives $\epsilon_{0°}(570) = 9 \times 10^4$ M^{-1} cm^{-1} for Arsenazo III molecules which are perfectly aligned along the horizontal axis, eqn. (9) with $\overline{\cos^2\gamma} = 1$.

0·3 mM are all similar and peak before tension. This is illustrated by the records in Fig. 8*A*, the last two records in Fig. 8*B*, the first record in Fig. 8*C*, and the records in Figs. 2 and 4 (shown by open squares in Fig. 9).

Resting Arsenazo III dichroism

Since the dichroic signal associated with an action potential appears to involve re-orientation of some of the dye molecules, it was important to find out whether Arsenazo III is oriented inside a resting fibre. Columns (5) and (6) of Table 2 give values of the difference in 0° and 90° absorbance at the isosbestic point, 570 nm (where dye absorbance is high), and at 720 or 750 nm (where dye absorbance is negligible and intrinsic dichroism is measured). The arithmetic difference between these values gives an estimate of dye-related dichroism at 570 nm and this is tabulated in column (7). The concentration of dye, if perfectly aligned along the fibre axis, which would give this amount of dichroism is indicated in column (8) (if the alignment were less complete, so that $\overline{\cos^2\gamma} < 1$, the required concentration would be greater). The average value of 4 μM in column (8) is not significantly different from zero, indicating that any net orientation of dye is small. If this were not the case, it would be necessary to use $[2A_{90°}(570)+A_{0°}(570)]/3$ in Beer's Law to estimate the concentration of dye in the radially symmetric muscle fibre (eqn. (12)). It will be seen later that the amount

of dye which participates in the dichroic signal may also be small; therefore, the failure to detect resting dichroism allows no conclusion regarding the resting state of the dye molecules that generate the dichroic signal.

Comparison of isotropic and dichroic signals during a train of action potentials

A rather interesting difference between the isotropic and dichroic signals was observed during a train of action potentials. The isotropic signal showed considerable

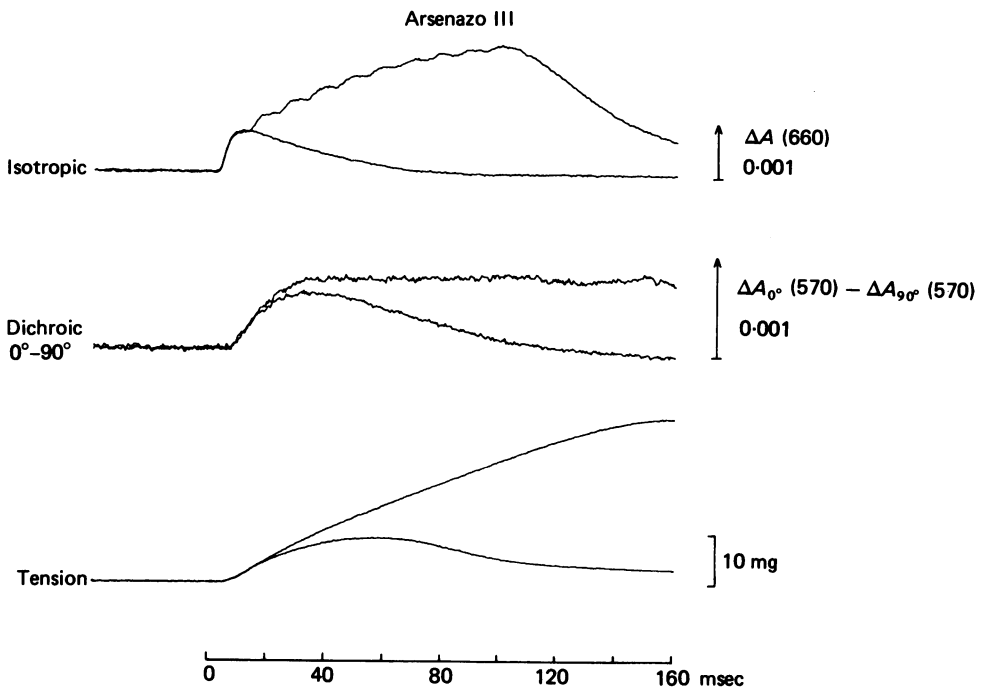

Fig. 10. Comparison of Arsenazo III isotropic and dichroic signals following both a single action potential and a train of action potentials. The upper traces show the 660 nm isotropic signals associated with one action potential and with ten action potentials spaced 10 msec apart. In this Figure an increase in absorbance is plotted in the upward direction. The middle traces show the 570 nm dichroic signals and the lower traces show tension. Tension continued to rise during the train, probably because of increasing amounts of overlap between thick and thin filaments at the contracting ends of the fibre. Dye-related $A(570) = 0{\cdot}035$ corresponding to 0·14 mM-dye. In this experiment a sampling interval of 0·4 msec was used throughout and was not changed to 2·0 msec after 250 points were collected. Same fibre as in Fig. 8*B*. The single action potential signals were signal averaged two to three times and the ten action potential signals were based on single sweeps.

summation whereas the dichroic signal rapidly reached a plateau level. This finding is illustrated by the experiment in Fig. 10. The top two superimposed records show the 660 nm isotropic signals following one and ten action potentials, plotted so that an increase in absorbance is an upward deflexion. The middle records show the 570 nm dichroic signals and the lower records show tension.

In this experiment the isotropic signal increased during the train so that following

the tenth action potential the magnitude was slightly more than three times as large as the peak magnitude associated with a single twitch. The dichroic signal, on the other hand, reached a plateau level only 30–40 % larger than the single twitch value. This point will be taken up again in the Discussion section where the possibility is considered that the dichroic signal depends on Ca^{2+} binding to high affinity myoplasmic Ca^{2+} receptors.

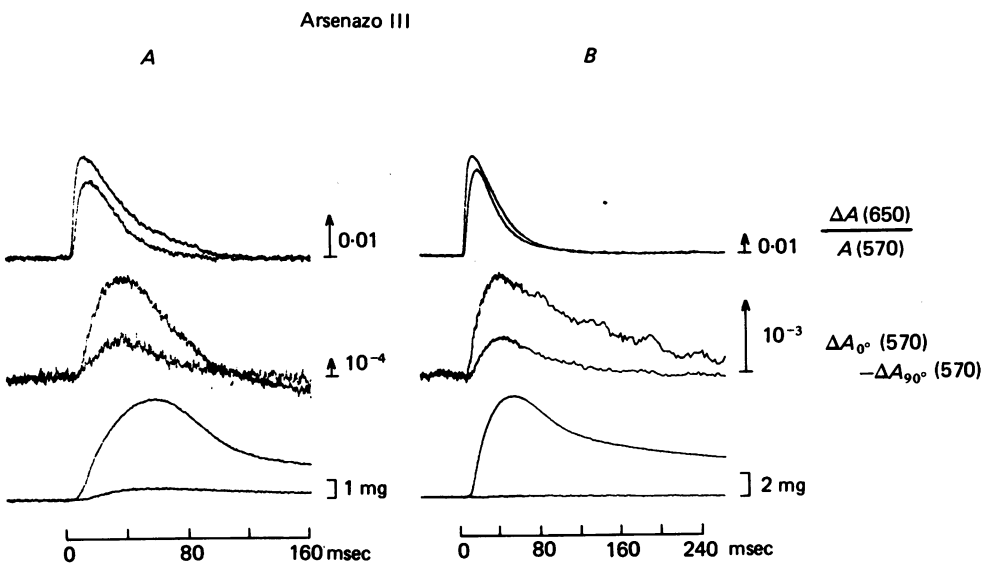

Fig. 11. Effect of D_2O and hypertonicity on Arsenazo III isotropic and dichroic signals. *A*, records of 650 nm isotropic signals (upper records), 570 nm dichroic signals (middle records) and tension (lower records). The larger magnitude records were taken in H_2O Ringer just before the solution change and the smaller magnitude records were taken in D_2O Ringer just after the change. Dye-related $A(570) = 0{\cdot}035$ corresponding to 0·14 mM-dye. Same fibre as shown in Fig. 8*B*. *B*, similar protocol to *A*. The larger magnitude records were taken in normal Ringer whereas the smaller magnitude records were taken in Ringer which was made to have approximately 2·5 times normal osmolality by adding 180 mM-NaCl. Dye-related $A(570)$ in normal Ringer was 0·079 corresponding to 0·25 mM-dye; dye-related $A(570)$ in the hypertonic solution was 0·064. Vertical diameter, 101 μm; horizontal diameter, 105 μm; sarcomere spacing, 3·6 μm; temperature, 14·9–15·8 °C; fibre 011979·1. In *A* and *B* the isotropic signals were signal averaged two to three times and the dichroic signals were differences of 0° and 90° records which were signal averaged one to five times.

Effects of D_2O and hypertonicity on the isotropic and dichroic signals

The preceding paper (Baylor *et al.* 1982*b*) showed that the Dichlorophosphonazo III dichroic signal was greatly suppressed when H_2O Ringer was replaced with D_2O Ringer. Fig. 11*A* shows the effects on the Arsenazo III signals which are produced by changing from H_2O Ringer to D_2O Ringer. The isotropic signals are the upper records, the dichroic signals are the middle records and tension records are lowermost. All three signals were depressed by D_2O but by different amounts. The isotropic signal was reduced to 75 % of its control value, the dichroic signal to 40 % of control value, and tension to 11 % of control value.

Fig. 11*B* shows that increasing the osmolality of Ringer from 1 × to 2·5 × normal reduces signal size in a manner somewhat similar to that shown for D_2O. The isotropic signal was reduced to 88 % of its control value, the dichroic signal to 38 % of control value, and tension to 1 % of control value. On return to normal Ringer recovery of all three signals was nearly complete (not shown).

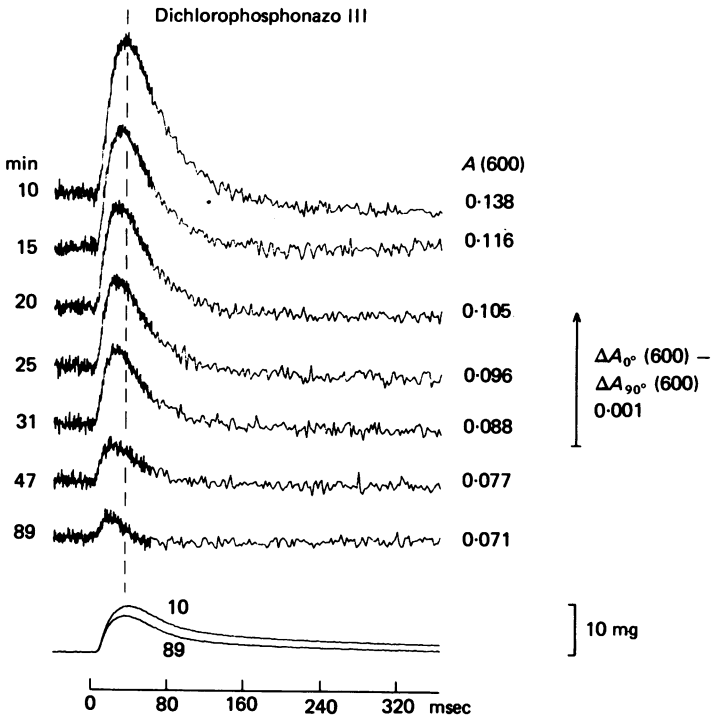

Fig. 12. Dichroic signals recorded from a fibre injected with Dichlorophosphonazo III. The seven optical traces were taken at different times, as indicated on the left, following completion of injection. Each $\Delta A_{0°}(600)$ and $\Delta A_{90°}(600)$ record which was used for the difference was signal averaged two times. Values of dye-related $A(600)$ are indicated on the right. The lowermost superimposed traces represent tension recorded during the first and last optical records. Vertical diameter, 98 μm; horizontal diameter, 122 μm; sarcomere spacing, 3·9 μm; Ringer, 15·6–15·9 °C. Fibre 070678·1.

Dichroic signals using Dichlorophosphonazo III

Dichroic signals are also readily seen in fibres injected with Dichlorophosphonazo III, a Ca^{2+} dye used by Brown, Cohen, De Weer, Pinto, Ross & Salzberg (1975) and by Yoshikami & Hagins (1978). Fig. 12 shows difference records which were taken as dye-related $A(600)$ decreased from 0·138 (corresponding to 0·27 mM-dye) to 0·071 (0·14 mM-dye). As the dye concentration decreased, the signal became progressively smaller. In addition, the first three records show a progressive decrease in time to peak.

Fig. 13 shows the variation of signal amplitude as a function of dye-related $A(600)$/cm or dye concentration, obtained from the experiment in Fig. 12 (○) and another fibre (□). Except for the data point farthest to the right, the dichroic signal

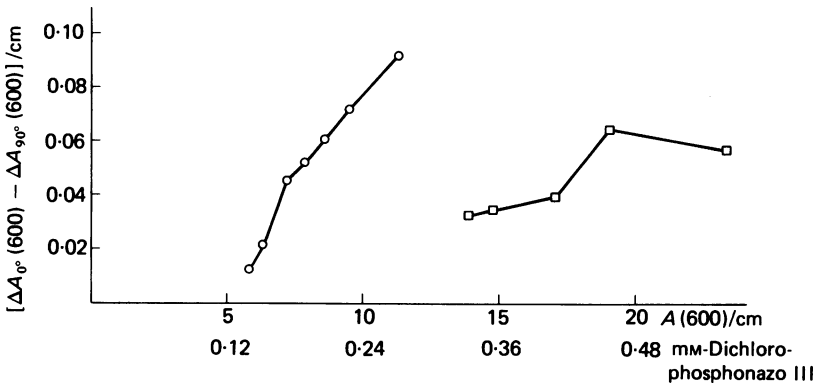

Fig. 13. Magnitude of the 600 nm dichroic signal in two fibres in which there were varying concentrations of Dichlorophosphonazo III. Abscissa gives dye-related $A(600)$ divided by fibre horizontal diameter on upper label and concentration of dye on the lower label. Ordinate gives peak values of the dichroic signal, corrected for the intrinsic dichroic signal and divided by fibre horizontal diameter. ○, from the experiment in Fig. 12. □, from fibre 070678·2; vertical diameter, 80 μm; horizontal diameter, 116 μm; sarcomere spacing, 3·9 μm; Ringer 15·9 °C.

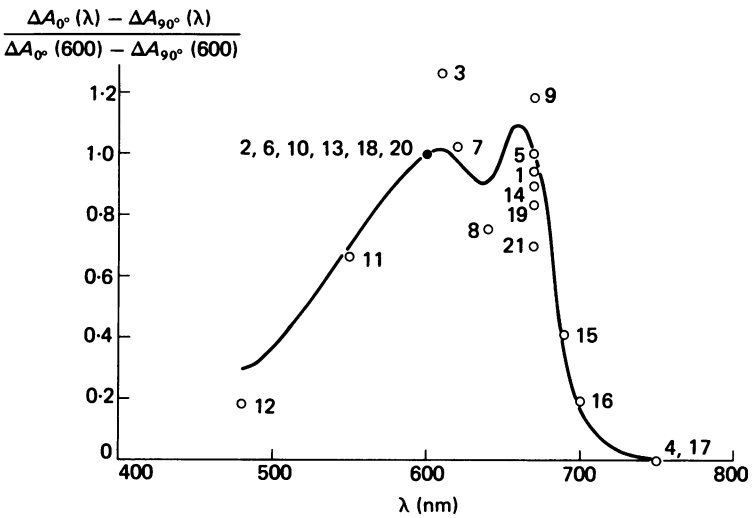

Fig. 14. Wavelength dependence of the amplitude of the Dichlorophosphonazo III dichroic signal. ○, peak amplitudes at different λ normalized by interpolated peak values at 600 nm, ●. The chronological order of measurements is indicated beside each symbol; the measurements at λ = 600 nm are shown in the first six records in Fig. 12. The curve is taken from Fig. 14 of Baylor *et al.* (1982*a*). It was determined from a cuvette measurement of a calibrating solution with $[Ca^{2+}] = 0$, $[Mg^{2+}] = 0{\cdot}216$ mM, pH = 6·9. Same fibre as in Fig. 12 of this paper and Fig. 14 of Baylor *et al.* (1982*a*).

in each fibre increased with increasing dye concentration. The Dichlorophosphonazo III dichroic signal shows a somewhat different dependence on dye concentration than does the Arsenazo III dichroic signal (compare Figs. 13 and 9).

Fig. 14 shows the amplitude of the dichroic signal plotted as a function of wavelength. In this experiment repeated measurements were made at 600 nm (first six

traces in Fig. 12) and interpolated values of the peak amplitude were used to normalize the peak values at other wavelengths. At all wavelengths the dichroic signal had the same temporal waveform as the bracketing 600 nm signals, indicating as with Arsenazo III that only one underlying process seems to be involved (although the process may change with time after injection).

The curve in Fig. 14 is taken from Fig. 14 of Baylor *et al.* (1982*a*) where it was shown to provide a reasonable fit to the resting Dichlorophosphonazo III spectrum in the same fibre. The curve also fits, as least to first approximation, the wavelength dependence of the amplitude of the dichroic signal.

The general conclusion is that a dichroic signal may be seen in fibres injected with Dichlorophosphonazo III and that this signal shows some similarities to the signal obtained with Arsenazo III. The polarity of both signals is the same; the onset of the dichroic signal occurs after the start of the Ca^{2+} signal (Baylor *et al.* 1982*b*); the peak of the signal precedes the peak of tension, at least with low dye concentration; the signal from both dyes shows the same waveform at all wavelengths; and the wavelength dependence of the amplitude of the signal resembles the resting absorbance spectrum of the dye. The two dichroic signals appear to have a different dependence on dye concentration, however, since with very low levels of Arsenazo III the dichroic signal is considerably greater than the Ca^{2+} signal whereas with small amounts of Dichlorophosphonazo III the Ca^{2+} signal is larger (Fig. 13 and Baylor *et al.* 1982*b*). Unfortunately, the isotropic signals obtained with Dichlorophosphonazo III are complex (Baylor *et al.* 1982*b*) and it is not possible to determine satisfactorily the individual contributions made by the 0° and the 90° signals to the total dichroic signal to see whether a change in dye orientation takes place.

Dichroic signals recorded using Arsenazo I and Antipyrylazo III

Dichroic signals of the same polarity as those described above were also observed in two experiments with Arsenazo I and in one experiment with Antipyrylazo III (high dye concentration), but they were small and were not studied in detail. However, the general time course preceded that for tension (measured with Arsenazo I) and lagged that for free $[Ca^{2+}]$ (measured with Antipyrylazo III), similar to the observations made with Arsenazo III and Dichlorophosphonazo III.

DISCUSSION

The Arsenazo III experiments reported in this paper indicate that at least two different kinds of changes in dye absorbance can be obtained from skeletal muscle fibres during activity. The earliest signal is isotropic and is mainly due to the formation of Ca^{2+}:dye complex in response to an increase in myoplasmic free $[Ca^{2+}]$ (Baylor *et al.* 1982*b*). The other, later signal is dichroic and appears to involve a change in orientation, and possibly a change in absorbance, of some of the dye molecules.

The identification of the second absorbance change as occurring in the re-orienting dye molecules is somewhat tentative. The results are equally consistent with a change in absorbance which occurs in another population of dye molecules at approximately the same time as the re-orientation dichroic signal. Since the presence of the second absorbance change is not very pronounced in heavily injected fibres, in which the isotropic signal predominates over the dichroic one (see p. 189),

it seems somewhat more economical to consider that the change in orientation and the temporally similar second change in absorbance occur in the same molecules.

The separation of the Arsenazo III signals into the two basic components was made possible because one component is dichroic and its waveform could be obtained by taking the difference between the absorbance changes measured with 0° and 90° light. If the same absorbance changes occurred in a cell possessing spherical symmetry, both components would be isotropic and it would not be possible to determine either one using this approach. In this case the optical signal would be composed of an early waveform, having the time course of the isotropic signal and spectral dependence shown in Fig. 3*C* or *D*, plus a late waveform, having the time course of the dichroic signal and the spectral dependence shown in Fig. 3*B*. The changes in dye absorbance which would be measured are those shown in Fig. 6*A*. This example illustrates the general principle that applies to radially symmetric structures such as a muscle fibre. If one wants to measure absorbance properties of dye molecules, either at rest of during activity, without effects of orientation, the measurement should use a 1:2 weighting for 0° and 90° light (eqns. (12), (13) and (24)).

An important question to consider is whether the dichroic signal seen with a small amount of Arsenazo III inside the fibre (no more than 0·2–0·3 mM) might simply by a dye-related 'artifact', related either to fibre movement or to the intrinsic dichroic signal seen in uninjected fibres (Baylor *et al.* 1982*a*). This seems unlikely for several reasons. The sign of the dye-related dichroic signal is opposite to the sign of the intrinsic dichroic signal and the waveforms of the two signals are quite different. Thus, the dye-related signal does not simply represent an amplification of the intrinsic signal. The dichroic signal, usually measured with spot illumination, was also present with whole-field illumination (not shown), which tended to give smaller movement-related signals than spot illumination. The effect of dye concentration on the signal appears to be complex (Figs. 8 and 9), whereas a dye-related artifact, on the simplest grounds, might be expected to increase in magnitude monotonically with dye concentration. D_2O and hypertonicity reduce both tension and the dichroic signal, but the effect on tension is much more marked, particularly in the hypertonic experiment (Fig. 11*B*). Finally, in the summation experiment, Fig. 10, the dichroic signal reached a plateau level whereas tension continued to increase.

A lower limit for the amount of Arsenazo III required to produce the dichroic signal

Two methods of calculation suggest that only a small fraction of the total dye present may participate in producing the dichroic signal. The first method for estimating the concentration, c, of dye which gives the dichroic signal can be obtained from Fig. 3*B*. The maximum change in $(\Delta A_{0°} + 2A_{90°})/3$ occurs at 600 nm and gives a value $0{\cdot}45 \times 10^{-3}$. According to eqn. (24) this corresponds to $A_2 - A_1$. Beer's Law states

$$A_2 - A_1 = (\epsilon_2 - \epsilon_1)\, cl, \tag{26}$$

in which $(\epsilon_2 - \epsilon_1)$ represents the change in molar extinction coefficient and l the path length, which for the fibre in Figs. 1–7 was 64 μm. Since it is highly unlikely that the change in molar extinction coefficient would exceed 3×10^4 M^{-1} cm^{-1} (Kendrick,

Ratzlaff & Blaustein, 1977), we can use this value as an upper limit to obtain a lower limit for c, calculated to be 2·3 μM.

Another method for calculating the lower limit for c is based on using the magnitude of $\Delta A_{0°}(570) - \Delta A_{90°}(570)$ which for the fibre is Figs. 1–7 was $0{\cdot}74 \times 10^{-3}$. According to eqn (25), if the re-orienting dye molecules underwent the largest possible change in orientation, from $\overline{\cos^2 \gamma_1} = 0$ to $\overline{\cos^2 \gamma_2} = 1$, and if 570 nm is an isosbestic wavelength for the absorbance change, $A_1(570) = A_2(570) = (2/9)(\Delta A_{0°} - \Delta A_{90°}) = 0{\cdot}000164$. Using $\epsilon(570) = 3 \times 10^4$ M^{-1} cm^{-1} and $l = 64$ μm, Beer's Law gives $c = 0{\cdot}85$ μM.

Thus, the two methods for calculating a lower limit for c give values of 2·3 and 0·85 μM which correspond to 1 % and 0·4 % of the total dye present in the experiment. In the first case, 2·3 μM dye molecules must undergo a change in orientation which, according to eqn. (25), should be $\overline{\cos^2 \gamma_2} - \overline{\cos^2 \gamma_1} = 0{\cdot}37$. In the second case, 0·85 μM dye molecules undergo the maximum possible change in orientation, $\overline{\cos^2 \gamma_2} - \overline{\cos^2 \gamma_1} = 1$. However, the experimental results are equally consistent with a situation in which more molecules undergo less change in orientation. In any case, it seems clear that the amount of dye which participates in the dichroic signal, and thus is probably unavailable to react with Ca^{2+}, may be small and its contribution to resting dichroism may be difficult to detect (Table 2).

Does the Arsenazo III dichroic signal arise from dye molecules which are associated with an oriented structure?

Since the Arsenazo III dichroic signal appears to involve a change in orientation of some of the dye molecules, one would expect the participating molecules either to be associated with (possibly bound to) one of the oriented structures in muscle or to be dissolved in myoplasm and be aligned by an orienting force (torque, to be precise). Three types of possible orienting forces come to mind: electrical, chemical and hydrostatic.

An example of an electrical force is the internal longitudinal voltage gradient which accompanies the action potential. A change in dye orientation could occur if either Arsenazo III or some of the proteins to which it is bound (Beeler, Schibeci & Martonosi, 1980) possesses a dipole moment. The difficulty with this idea is that the voltage gradient, which is proportional to the time derivative of the action potential, is brief and biphasic and precedes the Ca^{2+} signal (Miledi, Parker & Schalow, 1977) whereas the dichroic signal is long lasting and monophasic and lags the Ca^{2+} signal.

Another possibility is that a spatial gradient in voltage or chemical concentration, for example $[Ca^{2+}]$, might be present during activation and that this might influence the orientation of dye molecules. This case is difficult to evaluate in the absence of quantitative information concerning the gradient. However, using the simplest assumptions one might expect the magnitude of any resulting dichroic signal to be directly proportional to dye concentration and it is clear in Fig. 9 that this is not the case, at least for Arsenazo III.

Changes in dye orientation due to hydrostatic forces of fluid flow should also be kept in mind, although there is no reason to suppose that they are significant in the highly immobilized fibres which were used for these experiments. As was the case above, one might expect any resulting dichroic signal to depend linearly on dye concentration.

Although we are unable to rule out all the possibilities concerning orienting forces acting on dissolved dye molecules (possibly associated with soluble proteins), the most plausible explanation for the re-orienting dye molecules would seem to involve an association of the molecules with an oriented structure within the muscle fibre. The remainder of the Discussion section is concerned with various aspects of this kind of process. For simplicity, the association process will be described as though it involves sites on the structure which can bind dye molecules.

Does the change in orientation of dye molecules simply reflect a change in myoplasmic concentration of either free dye or Ca^{2+}-complexed dye?

One possibility to consider is whether the dichroic signal is a simple consequence of either the increase in concentration of Ca^{2+}-complexed dye or the decrease in concentration of free dye, changes which result from the increase in myoplasmic free $[Ca^{2+}]$. In this situation one could imagine that there are oriented binding sites for free dye (meaning Ca^{2+}-free dye in various protonated states, with and without Mg^{2+}; see Baylor *et al.* 1982*a*) or for Ca^{2+}-bound dye. These sites could be constant in number, always present, and might rapidly equilibrate with myoplasmic dye, so that the extent of occupancy would change as the concentration of the appropriate dye complex changed. The equilibration would need to involve a slight delay to account for the fact that the dichroic signal has a slower time course than the Ca^{2+} signal. The following arguments indicate that this explanation is unlikely to account for the dichroic signal.

First, consider the case for Ca^{2+}-free dye. One would suppose that Ca^{2+}-free dye is bound to oriented sites at rest and that during activity there is a decrease in the amount bound due solely to the decrease in myoplasmic Ca^{2+}-free dye. For this explanation to fit the data, the orientation of bound dye would need to favour absorption of 90° light, i.e. $\overline{\cos^2 \gamma_1} < 1/3$. During activity, some dye would leave the sites and become randomly oriented in the myoplasm, i.e. $\overline{\cos^2 \gamma_2} = 1/3$. In this situation the wavelength dependence of the magnitude of the dichroic signal, Fig. 3*A*, would correspond to the absorbance spectrum of the oriented bound dye molecules according to eqn. (25). This is plausible since the data in Fig. 3*A* are approximately fitted by the spectrum of Ca^{2+}-free Arsenazo III.

The difficulty with the hypothesis is that it fails to fit the experimental relationship between amplitude of the signal and free dye concentration. The clearest illustration of this is given by the summation experiment in Fig. 10. Suppose in the simplest situation that the amount of dye which is bound is directly proportional to myoplasmic free dye. Following a single action potential (Fig. 10) there should be a small decrease in concentration of Ca^{2+}-free dye which is given by the mirror image of the increase in concentration of Ca^{2+}:dye complex (isotropic signal). The dichroic signal would represent the corresponding decrease in oriented, bound dye. At the end of ten action potentials, the reduction in free dye was three times greater so that one would expect a three-fold increase in the dichroic signal. Instead, there was only a 30–40 % increase. The discrepancy becomes worse if one considers the more realistic possibility that the amount of dye bound is not directly proportional to free dye at all dye concentrations, but shows saturation.

The second possibility is that there are oriented sites for Ca^{2+}-complexed dye which become occupied when the concentration of Ca^{2+}-complexed dye increases. In this

case $\overline{\cos^2 \gamma_1} = 1/3$, $\overline{\cos^2 \gamma_2} > 1/3$, and the spectrum in Fig. 3*A* would correspond to the spectrum of the bound Ca^{2+}-complexed dye. Since the points in Fig. 3*A* are very different from the spectrum of Ca^{2+}:dye complex (see Fig. 1*A* of Baylor *et al.* 1982*b*), in particular at $\lambda = 660$ nm, it seems safe to exclude this possibility.

In conclusion, if the dichroic transient reflects the transient binding of dye to oriented sites, then such binding must result from a change in the oriented sites, brought about in the course of activity. For example, the oriented sites could undergo a change in affinity for Ca^{2+}-free dye. On the other hand, the participating dye molecules could be bound at rest and undergo a change in orientation during activity. In either case, an essential feature is that the dye-binding sites themselves must undergo change.

Time course of effects which might be produced by the myoplasmic Ca^{2+} transient

Since the results suggest that the Arsenazo III dichroic signal could reflect changes in oriented sites which can bind dye, the next question concerns the mechanism which might be responsible for altering the sites. One possibility is to suppose that the change in the binding sites is a result of the myoplasmic free $[Ca^{2+}]$ transient itself. For example, dye bound to one part of an oriented structure, such as thin filaments or the s.r. (sarcoplasmic reticulum), could have its orientation and absorbance spectrum changed by the binding of Ca^{2+} to a neighbouring Ca^{2+}-receptor site. The simplest kind of reaction between Ca^{2+} and its receptor site should follow

$$Ca^{2+} + S \underset{k_{-1}}{\overset{k_1}{\rightleftharpoons}} CaS, \tag{27}$$

with S and CaS representing unoccupied and occupied Ca^{2+}-receptor sites. Valence signs have been omitted from S and CaS. Changes in [CaS] follow

$$d[CaS]/dt = k_1[Ca^{2+}][S] - k_{-1}[CaS]. \tag{28}$$

$[Ca^{2+}]$ is taken to be zero at rest and to be directly proportional to the isotropic Arsenazo III signal during activity according to

$$[Ca^{2+}] = [Ca^{2+}]_p\, n(t). \tag{29}$$

$[Ca^{2+}]_p$ is the peak value of free $[Ca^{2+}]$ during a twitch and $n(t)$ is the normalized isotropic waveform (i.e. scaled to give a peak value of unity).

The assumption that $n(t)$ is directly proportional to free $[Ca^{2+}]$ seems reasonable for steady state conditions using either 1:1 or 1:2 stoichiometries for Ca^{2+}:dye complexation since the fraction of total dye which is complexed is always small. During the Ca^{2+} transient, the proportionality condition requires that the rate constant for Ca^{2+}:dye dissociation is rapid (Baylor *et al.* 1982*b*). Although there is no direct evidence bearing on this point, it seems to be a reasonable assumption since Arsenazo III, Antipyrylazo III and Dichlorophosphonazo III all appear to track myoplasmic free $[Ca^{2+}]$ with similar speed (Baylor *et al.* 1982*b*).

Both sides of eqn. (28) can be divided by [CaS] + [S], the total number of sites, so that the concentrations of occupied and unoccupied sites, [CaS] and [S], are reduced to fractional amounts $f(t)$ and $1 - f(t)$ respectively. Eqn (28) becomes

$$df/dt = k_1[Ca^{2+}]_p\, n(t)[1 - f(t)] - k_{-1} f(t) \tag{30}$$

$$= k_{-1}\left\{\frac{[Ca^{2+}]_p}{K_D}\, n(t)[1 - f(t)] - f(t)\right\}. \tag{31}$$

K_D the dissociation constant for the site, is equal to k_{-1}/k_1. This equation can be solved for $f(t)$ using the normalized Ca^{2+} transient $n(t)$ and any selected values for the two parameters k_{-1} and $[Ca^{2+}]_p/K_D$. In all the calculations possible radial and longitudinal non-uniformities in either concentrations or rate constants have been ignored.

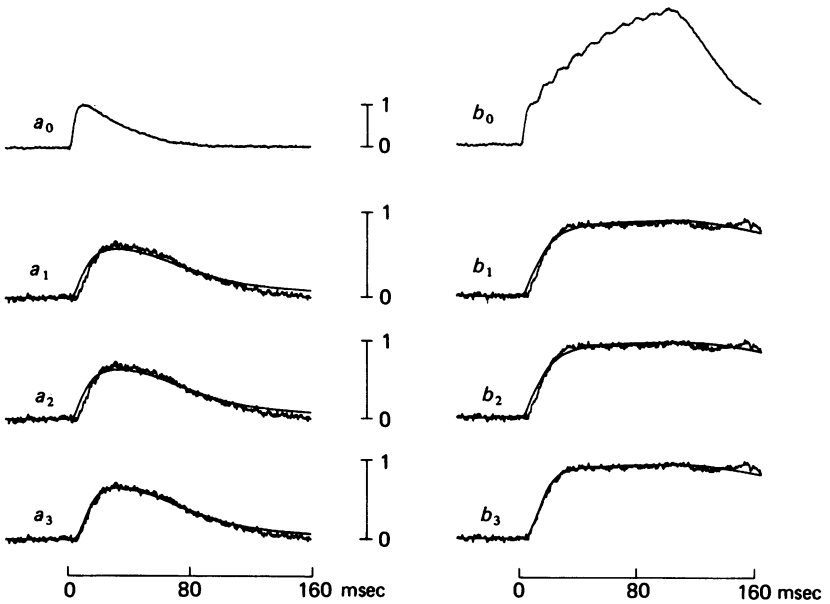

Fig. 15. Theoretical modelling of the Arsenazo III dichroic signal. From the experiment in Fig. 10. a_0 and b_0 show the Ca^{2+} waveforms following one and ten action potentials, divided by the peak value measured in trace a_0. (a_1, b_1), (a_2, b_2) and (a_3, b_3) show the three sets of theoretical curves, superimposed with the experimental dichroic curves, calculated for models (1), (2) and (3) using eqn. (31) and (a_0, b_0) for $n(t)$. The values for k_{-1} and $[Ca^{2+}]_p/K_D$ are given in Table 3. For each model the one and ten action potential records were fitted simultaneously and the pair of dichroic signals were scaled according to the factor given by the least squares fits. The single-twitch dichroic signal has been corrected for the intrinsic signal by subtracting the 750 nm signal scaled as $1/\lambda$; this correction elevated the signal slightly so that the final level was positive.

Three specific models relating the dichroic signal to $f(t)$ have been considered.

(1) Single site model. The dichroic signal is directly proportional to $f(t)$.

(2) Two site model, either of two occupancy. The dichroic signal is proportional to $2f(t)-f^2(t)$.

(3) Two site model, both of two occupancy. The dichroic signal is proportional to $f^2(t)$.

The first case is the easiest to consider and holds if the dichroic signal depends simply on the number of Ca^{2+}-receptor sites that are occupied. The next two cases concern receptors which have two identical Ca^{2+} sites which act independently, such as appears to be the case for the Ca^{2+}-regulatory sites on troponin (Potter & Gergely, 1975; Johnson, Robinson, Robertson, Schwartz & Potter, 1981) and may possibly be the case for the s.r. Ca^{2+} pump (cf. Tada, Yamamoto & Tonomura, 1978). Model (2) pertains to the situation in which the dichroic signal occurs if either or both sites

are occupied by Ca^{2+}. Model (3) requires that both sites be occupied for the dichroic signal to occur. In all three of the above cases it is assumed that there is negligible delay between the required binding of Ca^{2+} and the appearance of the dichroic signal.

Fig. 15 shows least squares computer modelling of the experiment in Fig. 10, using the three different models for relating the dichroic signal to $f(t)$. Traces a_0 and b_0 show

TABLE 3. Parameters used for the theoretical curves in Fig. 15

Model (1)	k_{-1} (sec^{-1}) (2)	$[Ca^{2+}]_p/K_D$ (3)	Relative standard deviation (4)	Peak fractional value of theoretical dichroic signal: Twitch (5)	Peak fractional value of theoretical dichroic signal: Train (6)
1	29·4	2·2	1·00	0·57	0·88
2	33·9	1·1	0·93	0·63	0·95
3	16·9	6·6	0·69	0·64	0·89

Column (1) refers to the model number described in the Discussion; column (2) gives the rate constant for Ca^{2+} leaving the hypothetical Ca^{2+}-receptor sites; column (3) gives the peak level of myoplasmic free $[Ca^{2+}]$ reached during a twitch, divided by the dissociation constant of the Ca^{2+}:receptor complex; column (4) gives the relative standard deviation of the difference between the experimental and theoretical curves. Columns (5) and (6) give the maximum values of the theoretical curves calculated for the single twitch and for the train of ten action potentials.

$n(t)$ following one and ten action potentials. The other records show superpositions of theoretical curves and scaled experimental dichroic records. Each theoretical curve shows the function of $f(t)$ which is appropriate for the particular model; $f(t)$ was obtained by numerical integration of eqn. (31) using a modified Runge-Kutta method (Romanelli, 1960). The values of k_{-1}, $[Ca^{2+}]_p/K_D$ and the scaling constant which relates the magnitude of the dichroic records to the appropriate function of $f(t)$ were adjusted to give a best least squares fit.

The second row in Fig. 15 (a_1, b_1) compares the computed and experimental traces using model (1) and the next rows use model (2) (a_2, b_2) and model (3) (a_3, b_3). All three models provide satisfactory fits, although model (3) provides the best fit and in particular reproduces the delay shown in the rising phase of the dichroic signal. Table 3 gives the various parameters associated with the theoretical fits.

The experiment illustrated in Fig. 15 is the only one in which we succeeded in making well bracketed measurements of the Ca^{2+} and dichroic signals during a train of action potentials. However, temporal comparison of the two waveforms was obtained in a number of single twitch experiments. In order to make theoretical fits to single twitch dichroic signals, it was necessary to arbitrarily set the scaling constant for the dichroic signal. For this purpose each dichroic signal was scaled so that the peak corresponded to 0·65 of maximum, in approximate agreement with the average peak of the experimental single twitch signals for all three models in Fig. 15 (traces a_1, a_2, a_3).

Table 4 shows values of k_{-1} and $[Ca^{2+}]_p/K_D$ obtained from the fitting of six single dichroic transients on five fibres in which Arsenazo III concentration was in the range 0·1–0·3 mM (see Fig. 9). The lower limit was set by the necessity of having enough

TABLE 4. Parameters used for single action potential fits

Fibre reference (1)	Dye (mM) (2)	Peak $\Delta A(650)/A(570)$ (3)	Model (1) k_{-1} (sec^{-1}) (4)	Model (1) $\frac{[Ca^{2+}]_p}{K_D}$ (5)	Model (2) k_{-1} (sec^{-1}) (6)	Model (2) $\frac{[Ca^{2+}]_p}{K_D}$ (7)	Model (3) k_{-1} (sec^{-1}) (8)	Model (3) $\frac{[Ca^{2+}]_p}{K_D}$ (9)
061478·1	0·24	0·019	20·8	2·9	24·9	1·2	13·3	7·6
	0·13	0·014	25·0	2·7	29·4	1·1	15·7	7·2
071378·1	0·23	0·037	12·0	3·9	14·2	1·6	7·1	10·7
010579·1	0·23	0·031	21·3	2·9	25·5	1·2	13·8	7·3
011979·1	0·27	0·061	11·7	4·1	13·8	1·7	7·1	11·0
012279·1	0·27	0·027	10·1	5·0	11·8	2·1	6·0	13·9
Average ± S.E.M.			16·8 ± 2·6	3·6 ± 0·4	19·9 ± 3·1	1·5 ± 0·2	10·5 ± 1·7	9·6 ± 1·1

Column (1) gives fibre reference, (2) gives Arsenazo III concentration and (3) gives peak $\Delta A(650)/A(570)$. The next colums give values of k_{-1} and $[Ca^{2+}]_p/K_D$ obtained from computer fits using model (1) (columns (4) and (5)), model (2) (columns (6) and (7)) and model (3) (columns (8) and (9)). For the fits the experimental dichroic signals were scaled to give a peak value of 0·65 (relative to a value of 1 which would correspond to $f = 1$ in eqn. (31)). When necessary, a small sloping base line correction was applied to the Ca^{2+} signal to ensure final return to 0 (Baylor *et al.* 1982*b*). When possible, the dichroic signals were corrected for the intrinsic dichroic signal. All records were fitted out to 260 msec after the stimulus, i.e. late into the falling phase of the dichroic signal. Temperature, 15·1–15·5 °C.

dye inside the fibre to produce a reliable isotropic signal. The upper limit was set by the finding that at higher dye concentrations the dichroic waveform developed an early, downward component (upper records in Fig. 8*B* and lower records in Fig. 8*C*).

The individual theoretical curves which were calculated from the six isotropic measurements provided good fits to the dichroic signals. The fits tabulated in the first three rows, Table 4, gave values of standard deviation in the sequence model (1) > model (2) > model (3) (i.e. model (3) gave the best fit) whereas the last three fits gave the reverse sequence. The differences between the two groups appeared to arise primarily because of differences in the signals during the falling phase, where any inexact correction for the intrinsic dichroic signal would become relatively more important. The model (3) curves always provided the best visual fit to the rising phase of the signals. On average the values of k_{-1} in Table 4 are about 0·6 times the values in Table 3 and the values of $[Ca^{2+}]_p/K_D$ are 1·4–1·6 times larger. Although the fractional constraint of 0·65 on the dichroic signal is somewhat arbitrary, the approximate agreement between Tables 3 and 4 indicates that the general features shown by the modelling in Fig. 15 are probably representative of all the experiments.

Conclusions from the modelling

The main conclusion which emerges from these calculations is that the dichroic signal can be satisfactorily explained on the assumption that Ca^{2+} binds to a Ca^{2+} receptor and that this binding changes the properties of Arsenazo III binding sites which are associated with the structure. On this basis reasonably good fits can be produced with either 1 Ca^{2+}- or 2 Ca^{2+}-site models, although the two site double occupancy model (3) provides the best description of the rising phase of the experimental records.

Although the modelling provides some quantitative information about the properties of the hypothetical Ca^{2+} sites, it does not provide precise identification. It is nevertheless natural to wonder whether any of the various Ca^{2+} receptors in muscle have Ca^{2+}-binding properties similar to those required for the hypothetical Ca^{2+} sites in the models (Tables 3 and 4). The values of the 'off' rate constant are model dependent and range from 6 to 33·9 sec^{-1}, with average values in Table 4 of 10·5–19·9 sec^{-1} (15 °C). This range is surprisingly close to the value for the Ca^{2+}-regulatory sites on whole rabbit troponin, 23 sec^{-1} at 25 °C, reported by Johnson *et al.* (1981).

The values of $[Ca^{2+}]_p/K_D$ are also model-dependent and lie within the range 1·1–13·9. In the previous paper (Baylor *et al.* 1982*b*) peak free $[Ca^{2+}]$ was estimated to be between 2 and 10 μM, giving estimates of K_D which vary from 0·14 to 9 μM. The average values in Table 4 give 0·6–2·8 μM for model (1), 1·3–6·7 μM for model (2) and 0·2–1·0 μM for model (3). For comparison, Potter & Gergely (1975) give $K_D = 0·2$ μM for whole rabbit troponin. In addition, they showed that the activation of myofibrillar ATPase by free $[Ca^{2+}]$ fitted the theoretical relationship derived on the assumption that two Ca^{2+} ions must be bound simultaneously to two Ca^{2+} receptors, analogous to model (3).

Thus, a possible mechanism for the dichroic signal would involve Ca^{2+} binding to troponin. Following binding there could be a change in the orientation and possibly absorbance of Arsenazo III molecules which are associated with either troponin or

some other part of the thin filament. If this idea is correct, the dichroic signal may reflect some aspect of thin filament activation.

However, this is not the only possibility which should be considered. As the analysis shows, any oriented structure which has a high affinity site for Ca^{2+}, with K_D in the range 0·1–1 times the peak free [Ca^{2+}], and an 'off' rate constant of 10–30 sec^{-1} at 15 °C is a viable candidate. Thus, another possibility to consider is the s.r. membrane system; this has a high affinity Ca^{2+}-binding site on the Ca^{2+} pump which may also have an 'off' rate constant of the required magnitude (Rauch, v. Chak & Hasselbach, 1978).

We are grateful to the staff of the electronic and machine shop in the Yale Department of Physiology for help with design and construction of equipment and to Dr D. R. Yingst for help with the purification of Arsenazo III. We are especially grateful to Dr L. B. Cohen for many useful discussions and suggestions. Helpful comments concerning the manuscript were made by R. W. Aldrich Jr., J. R. Chaillet, L. B. Cohen, M. Irving and J. G. Maylie. Financial support was provided by the American Heart Association (79–630, S.M.B.), the National Science Foundation (PCM 77-25163, S.M.B.), the Muscular Dystrophy Association (Grant to S.M.B. and fellowship to M.W.M.) and the U.S. National Institutes of Health (NS-07474, W.K.C.). S.M.B. is an Established Investigator of the American Heart Association.

REFERENCES

BAYLOR, S. M., CHANDLER, W. K. & MARSHALL, M. W. (1979*a*). Arsenazo III signals in singly dissected frog twitch fibres. *J. Physiol.* **287**, 23–24*P*.

BAYLOR, S. M., CHANDLER, W. K. & MARSHALL, M. W. (1979*b*). Arsenazo III signals in frog muscle. *Biophys. J.* **25**, 141a.

BAYLOR, S. M., CHANDLER, W. K. & MARSHALL, M. W. (1981). Comparison of optical signals in frog muscle obtained with three calcium indicator dyes. *Biophys. J.* **33**, 150a.

BAYLOR, S. M., CHANDLER, W. K. & MARSHALL, M. W. (1982*a*). Optical measurements of intracellular pH and magnesium in frog skeletal muscle fibres. *J. Physiol.* **331**, 105–137.

BAYLOR, S. M., CHANDLER, W. K. & MARSHALL, M. W. (1982*b*). Use of metallochromic dyes to measure changes in myoplasmic calcium during activity in frog skeletal muscle fibres. *J. Physiol.* **331**, 139–177.

BAYLOR, S. M. & OETLIKER, H. (1977). The optical properties of birefringence signals from single muscle fibres. *J. Physiol.* **264**, 163–198.

BEELER, T. J., SCHIBECI, A. & MARTONOSI, A. (1980). The binding of Arsenazo III to cell components. *Biochim. biophys. Acta* **629**, 317–327.

BROWN, J. E., COHEN, L. B., DE WEER, P., PINTO, L. H., ROSS, W. N. & SALZBERG, B. M. (1975). Rapid changes of intracellular free calcium concentration. *Biophys. J.* **15**, 1155–1160.

FREDERICQ, E. & HOUSSIER, C. (1973). *Electric Dichroism and Electric Birefringence*. Oxford: Clarendon Press.

HUXLEY, A. F. & PEACHEY, L. D. (1961). The maximum length for contraction in vertebrate striated muscle. *J. Physiol.* **156**, 150–165.

JOHNSON, J. D., ROBINSON, D. E., ROBERTSON, S. P., SCHWARTZ, A. & POTTER, J. D. (1981). Ca^{2+} exchange with troponin and the regulation of muscle contraction. In *The Regulation of Muscle Contraction: Excitation–Contraction Coupling*, ed. GRINNELL, A. D. & BRAZIER, M. A. B., pp. 241–257. New York: Academic Press.

KENDRICK, N. C., RATZLAFF, R. W. & BLAUSTEIN, M. P. (1977). Arsenazo III as an indicator for ionized calcium in physiological salt solutions: Its use for determination of the CaATP dissociation constant. *Analyt. Biochem.* **83**, 433–450.

MILEDI, R., PARKER, I. & SCHALOW, G. (1977). Measurement of calcium transients in frog muscle by the use of Arsenazo III. *Proc. R. Soc. Lond.* B **198**, 201–210.

POTTER, J. D. & GERGELY, J. G. (1975). The calcium and magnesium binding sites on troponin and their role in the regulation of myofibrillar adenosine triphosphatase. *J. biol. Chem.* **250**, 4628–4633.

RAUCH, B., v. CHAK, D. & HASSELBACH, W. (1978). An estimate of the kinetics of calcium binding and dissociation of the sarcoplasmic reticulum transport ATPase. *FEBS Letts* **93**, 65–68.

ROMANELLI, M. J. (1960). Runge-Kutta methods for the solution of ordinary differential equations. In *Mathematical Methods for Digital Computers*, vol. 1, ed. RALSTON, A., & WILF, H. S. pp. 110–120. New York: John Wiley.

TADA, M., YAMAMOTO, T. & TONOMURA, Y. (1978). Molecular mechanism of active calcium transport by sarcoplasmic reticulum. *Physiol. Rev.* **58**, 1–79.

YOSHIKAMI, S. & HAGINS, W. A. (1978). Calcium in excitation of vertebrate rods and cones: Retinal efflux of calcium studied with dichlorophosphonazo III. *Ann. N.Y. Acad. Sci.* **307**, 545–560.